AD-A185 434 EIGENVALUE PROJECTION THEORY FOR LINEAR OPERATOR EQUATIONS OF ELECTROMAGNETICS(U) ILLINOIS UNIV AT URBANA COORDINATED SCIENCE LAB A F PETERSON SEP 87 1/1

UNCLASSIFIED UILU-ENG-87-2252 N00014-84-C-0149 F/G 20/3 NL

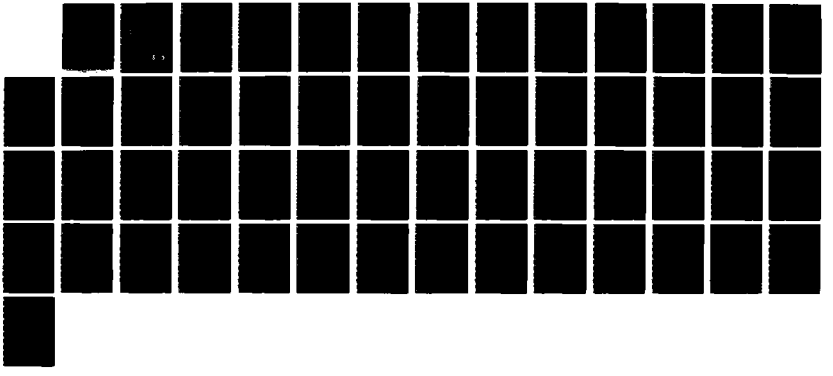

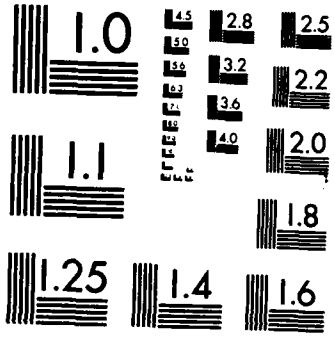

MICROCOPY RESOLUTION TEST CHART
NATIONAL BUREAU OF STANDARDS-1963-A

September 1987 UILU-ENG-87-2252

COORDINATED SCIENCE LABORATORY
College of Engineering

EIGENVALUE PROJECTION THEORY FOR LINEAR OPERATOR EQUATIONS OF ELECTROMAGNETICS

A. F. Peterson

UNIVERSITY OF ILLINOIS AT URBANA-CHAMPAIGN

UNCLASSIFIED
SECURITY CLASSIFICATION OF THIS PAGE

AD-A213 422

REPORT DOCUMENTATION PAGE

1a. REPORT SECURITY CLASSIFICATION Unclassified	1b. RESTRICTIVE MARKINGS None
2a. SECURITY CLASSIFICATION AUTHORITY	3. DISTRIBUTION/AVAILABILITY OF REPORT Approved for public release; distribution unlimited
2b. DECLASSIFICATION/DOWNGRADING SCHEDULE	
4. PERFORMING ORGANIZATION REPORT NUMBER(S) UILU-ENG-87-2252	5. MONITORING ORGANIZATION REPORT NUMBER(S)
6a. NAME OF PERFORMING ORGANIZATION Coordinated Science Lab University of Illinois 6b. OFFICE SYMBOL (If applicable) N/A	7a. NAME OF MONITORING ORGANIZATION Office of Naval Research
6c. ADDRESS (City, State, and ZIP Code) 1101 W. Springfield Ave. Urbana, IL 61801	7b. ADDRESS (City, State, and ZIP Code) 800 N. Quincy St. Arlington, VA 22217
8a. NAME OF FUNDING/SPONSORING ORGANIZATION Joint Services Electronics Program 8b. OFFICE SYMBOL (If applicable)	9. PROCUREMENT INSTRUMENT IDENTIFICATION NUMBER N00014-84-C-0149
8c. ADDRESS (City, State, and ZIP Code) 800 N. Quincy St. Arlington, VA 22217	10. SOURCE OF FUNDING NUMBERS PROGRAM ELEMENT NO. / PROJECT NO. / TASK NO. / WORK UNIT ACCESSION NO.

11. TITLE (Include Security Classification)
Eigenvalue Projection Theory for Linear Operator Equations of Electromagnetics

12. PERSONAL AUTHOR(S)
Peterson, A. F.

13a. TYPE OF REPORT	13b. TIME COVERED	14. DATE OF REPORT (Year, Month, Day)	15. PAGE COUNT
Technical	FROM _____ TO _____	September 1987	53

16. SUPPLEMENTARY NOTATION

17. COSATI CODES			18. SUBJECT TERMS (Continue on reverse if necessary and identify by block number)
FIELD	GROUP	SUB-GROUP	electromagnetic scattering, method of moments, matrix condition number, iterative methods

19. ABSTRACT (Continue on reverse if necessary and identify by block number)

Equations representing realistic electromagnetics problems seldom yield exact solutions and thus are usually treated numerically. In general, a discretization procedure such as the method of moments (also known as the weighted residual method) is used to convert the original continuous equation to a finite-dimensional matrix equation. A theory is presented that demonstrates the relation between the eigenvalue spectrum of the original, continuous operator and the eigenvalues of the method-of-moments matrix. In addition, an equivalence between the finite difference method and the method of moments is developed that permits the theory to be applied to finite-difference equations. Examples involving differential and integral equations are used to confirm the theory and to illustrate the typical eigenvalue spectrum arising in electromagnetic field problems.

20. DISTRIBUTION/AVAILABILITY OF ABSTRACT ☒ UNCLASSIFIED/UNLIMITED ☐ SAME AS RPT. ☐ DTIC USERS	21. ABSTRACT SECURITY CLASSIFICATION Unclassified
22a. NAME OF RESPONSIBLE INDIVIDUAL	22b. TELEPHONE (Include Area Code) / 22c. OFFICE SYMBOL

DD FORM 1473, 84 MAR — 83 APR edition may be used until exhausted. All other editions are obsolete.

SECURITY CLASSIFICATION OF THIS PAGE
UNCLASSIFIED

EIGENVALUE PROJECTION THEORY

FOR LINEAR OPERATOR EQUATIONS OF ELECTROMAGNETICS

A. F. Peterson

ABSTRACT

Equations representing realistic electromagnetics problems seldom yield exact solutions, and thus are usually treated numerically. In general, a discretization procedure such as the method of moments (also known as the weighted residual method) is used to convert the original continuous equation to a finite-dimensional matrix equation. A theory is presented that demonstrates the relation between the eigenvalue spectrum of the original, continuous operator and the eigenvalues of the method-of-moments matrix. In addition, an equivalence between the finite difference method and the method of moments is developed that permits the theory to be applied to finite-difference equations. Examples involving differential and integral equations are used to confirm the theory and to illustrate the typical eigenvalue spectrum arising in electromagnetic field problems.

KEY WORDS: electromagnetic scattering, method of moments, matrix condition number, iterative methods.

TABLE OF CONTENTS

Page

1. INTRODUCTION 1

2. EIGENVALUE PROJECTION THEORY 3

3. DISCRETIZATION PROCEDURES FOR CONTINUOUS EQUATIONS 6

4. SOME CONTINUOUS OPERATORS AND THEIR EIGENVALUES 14

5. EIGENVALUE SPECTRUM OF MATRIX OPERATORS 36

6. APPLICATIONS OF THE EIGENVALUE PROJECTION THEORY TO MATRIX CONDITIONING AND THE CONVERGENCE OF ITERATIVE ALGORITHMS 44

7. CONCLUSIONS 47

8. REFERENCES 48

1. INTRODUCTION

The treatment of realistic electromagnetic scattering problems is usually beyond the scope of exact analytical techniques. Instead, discretization procedures such as the finite difference method (FDM)[1], the finite element method (FEM)[2], and the method of moments (MoM)[3] (also known as the weighted residual method) are used to convert the original continuous equation to a finite-dimensional matrix equation. The solution of the matrix equation may be obtained from a straightforward application of direct algorithms such as Gaussian elimination, unless the system is of large order or happens to be poorly conditioned. In the latter situations, preconditioned iterative methods may offer advantages over direct algorithms[4].

Iterative algorithms usually converge at a rate that is highly dependent upon the eigenvalue spectrum of the system matrix[4,5]. This eigenvalue spectrum is related in turn to the eigenvalue spectrum of the original continuous operator, and to the specific discretization procedure (i.e., basis and testing functions) used to construct the matrix equation. Information about the eigenvalue spectrum enables the selection of a convergent iterative algorithm, and may be helpful for identifying optimal parameters to accelerate the convergence of iterative algorithms.

This report presents a theory delineating the relationship of the eigenvalues of the continuous operator to those of the matrix operator. If the spectrum of the continuous operator is known, the theory can be used to judge the effects of specific basis and testing functions on the eigenvalue spectrum and condition of the matrix. If the spectrum is unknown, the eigenvalues of the

matrix can be used to estimate the eigenvalue spectrum of the continuous operator, which may promote a better understanding of the continuous equations representing a physical problem. For example, it will be shown in Chapter 4 that the eigenvalue spectrum of the magnetic-field integral equation (MFIE) is fundamentally different from that of the electric-field integral equation (EFIE), which helps to explain why certain iterative algorithms are successful at treating the MFIE but not the EFIE.

Chapter 2 presents the theory linking the eigenvalues of the continuous operator with those of the matrix. This theory involves the explicit use of the MoM discretization procedure, and may not appear to be directly applicable to matrix equations constructed using the FEM or FDM procedures. Chapter 3 addresses the relationship between the different discretization procedures, and shows that both the FEM and the FDM can be interpreted in the context of the MoM. Therefore, the theory developed for MoM matrices can also be applied to finite-difference matrices and finite-element matrices. Chapter 4 presents a variety of continuous operators whose eigenvalue spectrums are available from analytical manipulation. All of the examples involve scalar equations with discrete spectrums. Chapter 5 compares the eigenvalues from the examples of Chapter 4 to numerical results, in order to confirm the theory and illustrate some of its applications. Additional applications are discussed in Chapter 6.

2. EIGENVALUE PROJECTION THEORY

Consider a continuous linear operator equation of the form

$$L\, f = g \tag{2.1}$$

where f is an unknown function to be determined and g is a specified excitation. In practice, the analytical inversion of Equation (2.1) may not be possible. However, an approximate solution may be obtained in terms of the finite expansion

$$f \approx \sum_{n=1}^{N} a_n B_n \tag{2.2}$$

where the basis functions B_n are specified and the coefficients a_n are unknowns to be determined. The equation can be enforced approximately in terms of the testing functions T_m, producing a discrete system of the form

$$\sum_{n=1}^{N} a_n \langle T_m, L\, B_n \rangle = \langle T_m, g \rangle \qquad m = 1, 2, \ldots, N \tag{2.3}$$

where the brackets denote a suitably defined inner product[3]. This matrix equation can be written

$$\underline{\underline{L}}\, \underline{a} = \underline{h} \tag{2.4}$$

where the elements of the matrix L are

$$\ell_{mn} = \langle T_m, L\, B_n \rangle \tag{2.5}$$

and the elements of the right-hand side are

$$h_m = \langle T_m, g \rangle \tag{2.6}$$

The process of expanding the unknown function f and enforcing Equation (2.1) approximately is known as the method of moments (MoM). The theory presented here is similar to that developed in Chapter 7 of [3].

The eigenvalues of the continuous operator L can be found from the solution of the eigenvalue equation

$$L\,\varepsilon = \lambda\,\varepsilon \tag{2.7}$$

where ε denotes an eigenfunction and λ the corresponding eigenvalue. If the above MoM discretization procedure is applied to the eigenvalue equation, the unknown eigenfunctions become

$$\varepsilon \approx \sum_{n=1}^{N} e_n\,B_n \tag{2.8}$$

and Equation (2.7) reduces to

$$\sum_{n=1}^{N} e_n \langle T_m, L\,B_n \rangle = \lambda \sum_{n=1}^{N} e_n \langle T_m, B_n \rangle \qquad m = 1, 2, \ldots, N \tag{2.9}$$

This discrete system can be written as a matrix equation

$$\underline{\underline{L}}\;\underline{e} = \lambda\;\underline{\underline{S}}\;\underline{e} \tag{2.10}$$

where the elements of the matrix $\underline{\underline{L}}$ are

$$\ell_{mn} = \langle T_m, L\,B_n \rangle \tag{2.11}$$

and the elements of the matrix $\underline{\underline{S}}$ are

$$S_{mn} = \langle T_m, B_n \rangle \tag{2.12}$$

Assuming the matrix $\underline{\underline{S}}$ in nonsingular, Equation (2.12) can be rearranged to yield

$$\underline{\underline{S}}^{-1} \underline{\underline{L}} \, \underline{e} = \lambda \, \underline{e} \tag{2.13}$$

Thus, the eigenvalues λ from Equation (2.13) should approximate those of Equation (2.1). The latter is a finite-dimensional matrix equation and will yield at most N independent eigenvalues. The continuous operator will, in general, yield an infinite number of eigenvalues. However, in some sense the dominant eigenvalues of the original operator should be approximated by the eigenvalues of the matrix operator $\underline{\underline{S}}^{-1} \underline{\underline{L}}$. In addition, the corresponding eigenfunctions should be approximated by the expansion

$$\varepsilon \approx \sum_{n=1}^{N} e_n B_n \tag{2.14}$$

where e_n are the elements of the eigenvectors of the matrix $\underline{\underline{S}}^{-1} \underline{\underline{L}}$.

The above theory is presented in the context of the MoM discretization, and may not seem directly applicable to finite-difference or finite-element matrices. To show that these relationships can be applied to finite-difference and finite-element systems, Chapter 3 discusses an equivalence between the three discretization procedures. Subsequent chapters address the verification of the theory using examples from electromagnetics.

3. DISCRETIZATION PROCEDURES FOR CONTINUOUS EQUATIONS

The previous chapter introduced the method of moments (MoM) discretization procedure[3]. The MoM requires the explicit introduction of basis and testing functions in order to discretize the domain and range spaces of the continuous operator. Other widely-used discretization procedures include the finite-element method (FEM)[2] and finite-difference method (FDM)[1]. This chapter shows an equivalence between the FEM, FDM, and MoM procedures for several simple examples.

The FEM has its origin in the works of Rayleigh and Ritz (1908) who developed an approximate procedure for estimating the minimum value of a quadratic functional and the function that attained this value[6]. The Russian scientists I. G. Bubnov (1913) and B. G. Galerkin (1915) observed that the equations obtained by the Ritz procedure could also be obtained directly, i.e., without regard to the minimization of a functional[6]. The general procedure they developed for the approximate solution of any continuous operator equation is essentially the MoM.

Because of the relationship between the minimization of a functional by the Ritz procedure and Galerkin's method, the FEM and the MoM are often equivalent procedures. The FDM is not based on the same concepts, and cannot be made exactly equivalent to the MoM. However, the FDM can be interpreted as an approximation to the MoM, at least to dominant order. In other words, basis and testing functions can be found that create a MoM matrix that closely approximates the FDM matrix. Specific examples are presented below to demonstrate this equivalence for FEM and FDM matrices.

The two-dimensional Helmholtz wave equation can be written

$$\frac{\partial^2 f}{\partial x^2} + \frac{\partial^2 f}{\partial y^2} + k^2 f(x,y) = g(x,y) \tag{3.1}$$

where g is some given excitation and f is the unknown function to be determined. For vanishing Dirichlet boundary conditions (i.e., $f(x,y) = 0$ on the boundary of the region of interest), the solution to Equation (3.1) is the function that minimizes the functional[2]

$$F(f) = \frac{1}{2} \iint \left\{ |\nabla f|^2 - k^2 f^2 + 2gf \right\} dxdy \tag{3.2}$$

The basic idea behind the Ritz procedure and the FEM is to expand the unknown function f in terms of trial functions according to

$$f(x,y) \approx \sum_{n=1}^{N} a_n B_n (x,y) \tag{3.3}$$

This expansion is substituted into Equation (3.2), replacing the original functional by one that now depends on the N unknown coefficients $a_1, a_2, a_3, \ldots a_N$.

If the functional is differentiated with respect to each of the unknown coefficients, and the result equated to zero in order to describe the stationary point, the process yields the discrete system

$$\sum_{n=1}^{N} a_n \iint \left\{ \nabla B_m \cdot \nabla B_n - k^2 B_m B_n \right\} dxdy = - \iint B_m g \, dxdy \tag{3.4}$$

$$m = 1, 2, \ldots, N$$

This can be written as a matrix equation

$$\underline{\underline{L}}\, \underline{a} = \underline{h} \tag{3.5}$$

where the elements of the matrix $\underline{\underline{L}}$ are

$$\ell_{mn} = \iint \{\nabla B_m \cdot \nabla B_n - k^2 B_m B_n\} \, dxdy \tag{3.6}$$

and the elements of the right-hand side are

$$h_m = - \iint B_m \, g \, dxdy \tag{3.7}$$

Consider a direct application of the MoM to Equation (3.1), again for the case of vanishing Dirichlet boundary conditions. If the function f is replaced by an expansion of the form identical to that appearing in Equation (3.3), and testing functions $T_m(x,y)$ are used to enforce the equation approximately, the result can be written

$$\sum_{n=1}^{N} a_n \iint \{T_m \nabla^2 B_n + k^2 T_m B_n\} \, dxdy = \iint T_m \, g \, dxdy \tag{3.8}$$
$$m = 1, 2, \ldots, N$$

If integration by parts is used to reduce the order of the derivatives appearing in Equation (3.8), the result is the discrete system

$$\sum_{n=1}^{N} a_n \iint \{\nabla T_m \cdot \nabla B_n - k^2 T_m B_n\} \, dxdy = - \iint T_m \, g \, dxdy \tag{3.9}$$
$$m = 1, 2, \ldots, N$$

This system is obviously a generalization of that appearing in Equation (3.4). If the testing functions are taken to be identical to the basis functions, this discrete system is identical with that produced by the functional minimization procedure.

The above comparison suggests that the FEM discretization procedure is equivalent to the MoM procedure. The FDM is not exactly equivalent to the MoM, but an approximate equivalence can be shown. For instance, consider the one-dimensional wave equation

$$\frac{d^2f}{dx^2} + k^2 f(x) = g(x) \tag{3.10}$$

The conventional central-difference formulas lead to the matrix equation[1]

$$\underline{\underline{L}}\,\underline{a} = \underline{h} \tag{3.11}$$

where

$$\ell_{mn} = \begin{cases} -\frac{2}{\Delta^2} + k^2 & m = n \\ \frac{1}{\Delta^2} & m = n \pm 1 \\ 0 & \text{other} \end{cases} \tag{3.12}$$

and

$$h_m = g(x_m) \tag{3.13}$$

The interval size Δ is assumed constant.

Now, consider the same equation in the context of the MoM. If the basis functions

$$B_n(x) = t(x;\ x_n - \Delta,\ x_n,\ x_n + \Delta) \tag{3.14}$$

and testing functions

$$T_m(x) = \frac{1}{\Delta}\, p(x;\ x_m - \frac{\Delta}{2},\ x_m + \frac{\Delta}{2}) \tag{3.15}$$

are used to discretize Equation (3.9) according to the MoM (these functions are defined in Figure 3.1), the matrix elements of Equation (3.11) are given by

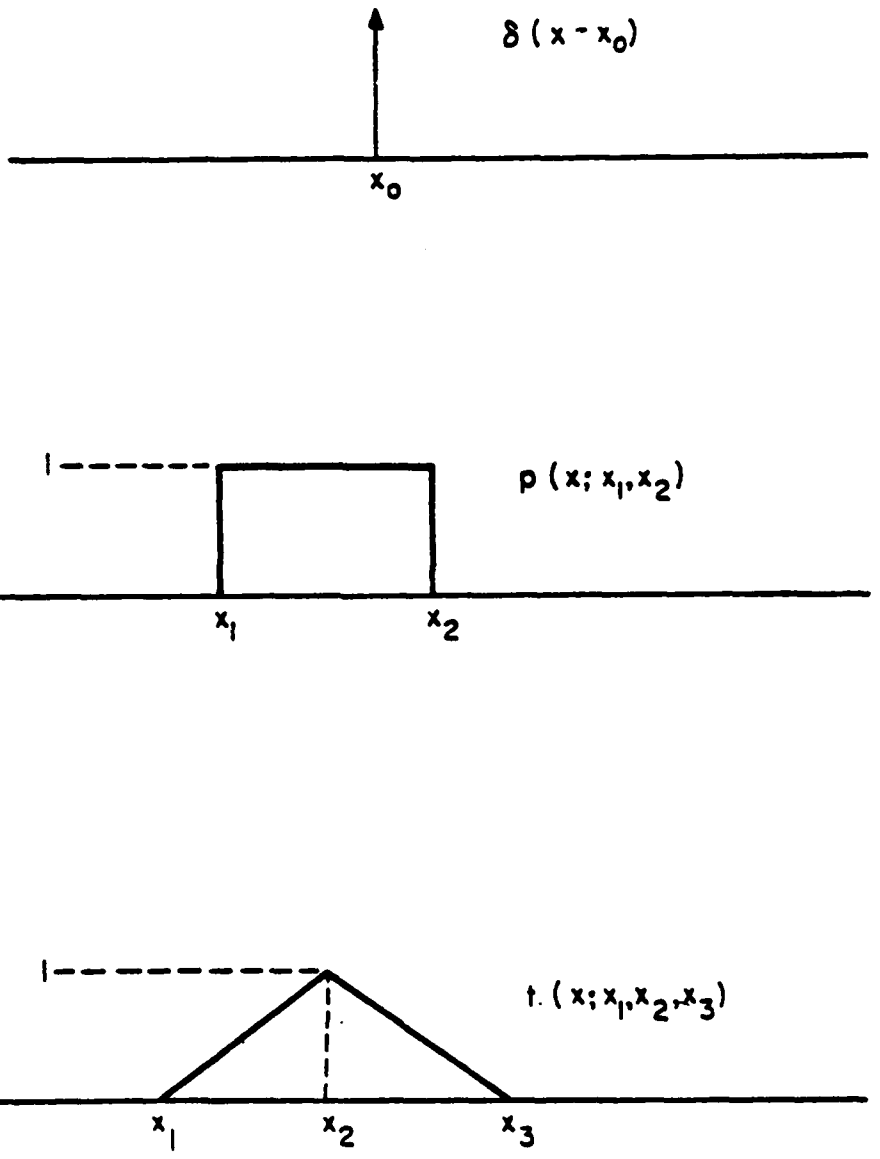

Figure 3.1 Definition of the subsectional basis and testing functions used in one-dimensional problems.

$$\ell_{mn} = \begin{cases} -\frac{2}{\Delta^2} + \frac{3}{4}k^2 & m = n \\ \frac{1}{\Delta^2} + \frac{1}{8}k^2 & m = n \pm 1 \\ 0 & \text{other} \end{cases} \tag{3.16}$$

and

$$h_m = \frac{1}{\Delta}\int_{x_m - \Delta/2}^{x_m + \Delta/2} g(x)dx \tag{3.17}$$

Note that Equations (3.16) and (3.17) agree to dominant order with Equations (3.12) and (3.13), i.e., as $\Delta \to 0$. Since neither of the above expressions are exact except in the limit of vanishing Δ, Equations (3.16) and (3.17) may be as legitimate as the central-difference formulas presented in Equations (3.12) and (3.13). For small values of Δ these matrices are virtually identical.

Now, consider the two-dimensional wave equation

$$\frac{\partial^2 f}{\partial x^2} + \frac{\partial^2 f}{\partial y^2} + k^2 f(x,y) = g(x,y) \tag{3.18}$$

The conventional central-difference approach yields the discrete operator with

$$\ell_{mn} = \begin{cases} -\frac{4}{\Delta^2} + k^2 & m = n \\ \frac{1}{\Delta^2} & \text{m, n represents adjacent grid points} \\ 0 & \text{otherwise} \end{cases} \tag{3.19}$$

$$h_m = g(x_m, y_m) \tag{3.20}$$

If the MoM procedure is used with the modified pyramid basis functions defined in Figure 3.2, i.e.,

$$B_n(x,y) = MP\ (x_n,\ y_n,\ \Delta) \tag{3.21}$$

and

$$T_m(x,y) = \frac{1}{\Delta^2}\, p(x;\ x_m - \tfrac{\Delta}{2},\ x_m + \tfrac{\Delta}{2})\ p(y;\ y_m - \tfrac{\Delta}{2},\ y_m + \tfrac{\Delta}{2}) \tag{3.22}$$

the elements of the discrete operator are given by

$$\ell_{mn} = \begin{cases} -\dfrac{4}{\Delta^2} + \dfrac{7k^2}{12} & m = n \\ \dfrac{1}{\Delta^2} + \dfrac{k^2}{12} & m,\ n \text{ represent adjacent grid points} \\ k^2/48 & m,\ n \text{ represent adjacent corner grid points} \\ 0 & \text{otherwise} \end{cases} \tag{3.23}$$

$$h_m = \frac{1}{\Delta^2} \int_{x_m - \Delta/2}^{x_m + \Delta/2} \int_{y_m - \Delta/2}^{y_m + \Delta/2} g(x,y)\, dxdy \tag{3.24}$$

Again, the discrete operator produced by the MoM agrees with the operator produced by the conventional FDM, at least in the limiting case $\Delta \to 0$.

This chapter demonstrates that the FEM and FDM discretizations can be interpreted in the context of the MoM, and thus can also be studied within the scope of the eigenvalue projection theory of Chapter 2. Subsequent chapters will compare theoretical eigenvalues to those of the finite-difference and MoM matrices in order to verify this theory.

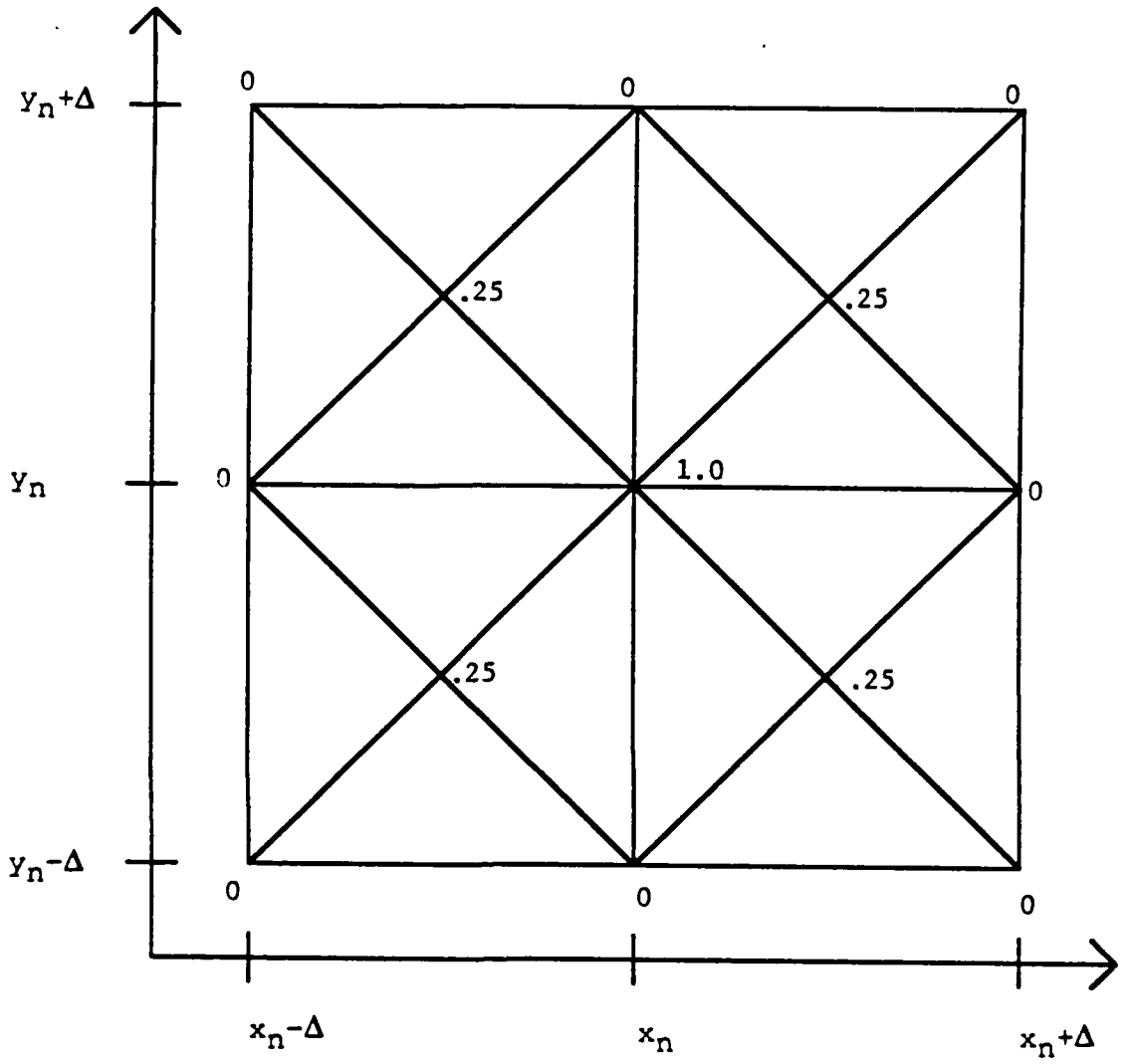

Figure 3.2 Top view of the modified pyramid function $MP(x_n, y_n, \Delta)$. The function is piecewise linear in x and y, and vanishes outside the domain $x_n - \Delta < x < x_n + \Delta$. $y_n - \Delta < y < y_n + \Delta$. Values at inflection points are shown.

4. SOME CONTINUOUS OPERATORS AND THEIR EIGENVALUES

4.1 Introduction

This chapter presents several examples for which the eigenvalues of continuous operators are readily available analytically. Initially, differential operators of the Laplace and Helmholtz type are considered. These are frequently used in connection with FDM or FEM discretizations. Subsequently, we examine the operators of the electric-field integral equation (EFIE), the magnetic-field integral equation (MFIE), and the combined-field integral equation (CFIE) for electromagnetic scattering from conducting bodies. These equations have been used extensively to represent external scattering problems. All of the examples presented here are two-dimensional in nature, i.e., they represent idealized structures that are infinitely long or have no variation in the third dimension. The equations involved are scalar equations. For each example, we identify the operator and the corresponding eigenfunctions and eigenvalues according to the equation

$$L\,\epsilon = \lambda\,\epsilon \tag{4.1}$$

where L denotes the continuous operator, ϵ an eigenfunction, and λ the corresponding eigenvalue. The continuous operators under consideration in this chapter all possess a discrete spectrum, i.e., an infinite number of discrete eigenvalues. In Chapter 5, these same examples are investigated numerically to show the connection between the continuous operator and the matrix operator.

4.2 Poisson's equation for a grounded rectangular cylinder

Consider a grounded conducting cylinder of rectangular shape, containing some given distribution of time-invariant electric charge density. The cross-sectional geometry is shown in Figure 4.1, where a and b are the rectangle dimensions. The electric potential $\phi(x,y)$ must satisfy the Poisson equation

$$\frac{\partial^2\phi}{\partial x^2} + \frac{\partial^2\phi}{\partial y^2} = g(x,y) \qquad 0 < x < a,\ 0 < y < b \tag{4.2}$$

where $g(x,y)$ represents the given charge distribution, scaled to give proper units. Since the rectangular cylinder is grounded, the potential must vanish everywhere on the cylinder. Thus, the eigenfunctions of the differential operator

$$L_{POISSON}(\phi) = -\frac{\partial^2\phi}{\partial x^2} - \frac{\partial^2\phi}{\partial y^2} \tag{4.3}$$

are

$$\epsilon_{mn} = \sin\left(\frac{m\pi y}{b}\right) \sin\left(\frac{n\pi x}{a}\right) \qquad n,\ m > 0 \tag{4.4}$$

and it is easily verified that the eigenvalues for this case are

$$\lambda_{mn} = \left(\frac{m\pi}{b}\right)^2 + \left(\frac{n\pi}{a}\right)^2 \tag{4.5}$$

Note that the operator is positive definite, that is, all the eigenvalues are real-valued and positive. Some of the smaller eigenvalues are presented in Table 4.1.

The eigenvalues depend on the dimensions of the cylinder, and as the cylinder is made larger they tend to decrease in value. As the cylinder is made

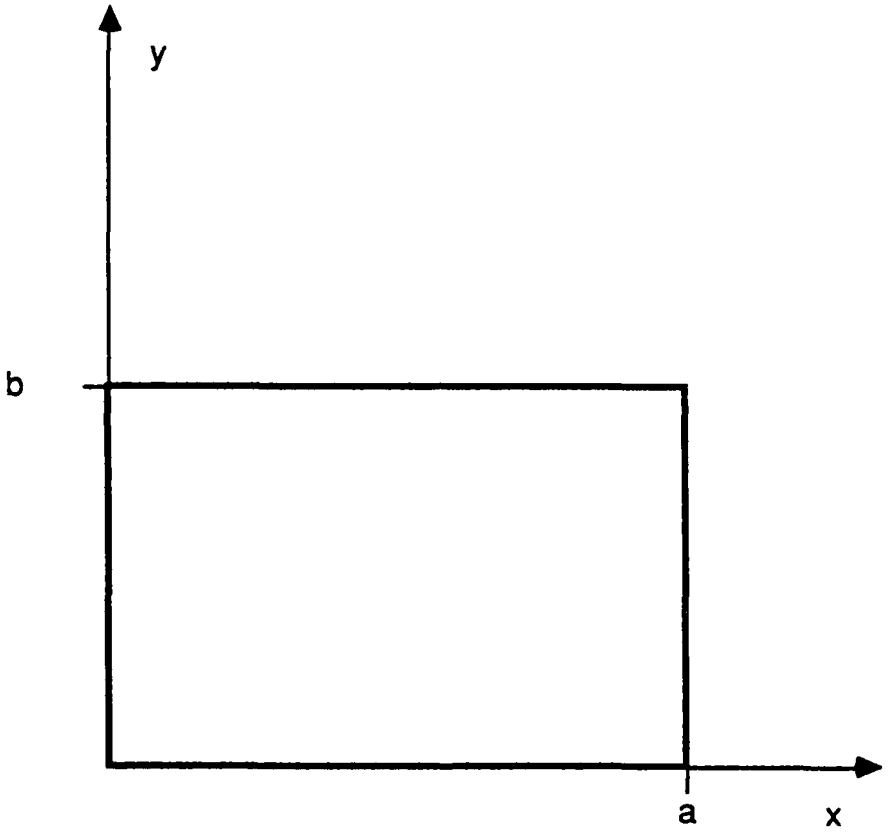

Figure 4.1 Geometry of grounded rectangular cylinder.

TABLE 4.1

EIGENVALUES OF THE POISSON OPERATOR APPLIED TO A GROUNDED RECTANGULAR CYLINDER, a = 2, b = 1.

m	n	λ_{mn}
1	1	12.337
1	2	19.739
1	3	32.076
2	1	41.946
1	4	49.348
2	2	49.348
2	3	61.685
1	5	71.555

smaller, they move away from the origin. For any size cylinder, there are an infinite number of eigenvalues with values greater than any finite number. In a loose sense, we can say that they tend to cluster at infinity.

4.3 Helmholtz' equation for a grounded rectangular cylinder

If the source terms in the previous example varied with time in a sinusoidal manner, the potential within the grounded rectangular cylinder would satisfy the wave equation

$$\frac{\partial^2\psi}{\partial x^2} + \frac{\partial^2\psi}{\partial y^2} + k^2\psi(x,y) = h(x,y) \qquad (4.6)$$

where h(x,y) represents the excitation, scaled to proper units. Assume that the wavenumber 'k' is real-valued, and proportional to the reciprocal of the wavelength. The potential ψ must vanish on the cylinder walls. In this case, the differential operator can be written

$$L_{HELMHOLTZ}(\psi) = -\frac{\partial^2\psi}{\partial x^2} - \frac{\partial^2\psi}{\partial y^2} - k^2\psi \qquad (4.7)$$

The eigenfunctions of this operator are the functions

$$\varepsilon_{mn}(x,y) = \sin\left(\frac{m\Pi y}{b}\right) \sin\left(\frac{n\Pi x}{a}\right) \qquad (4.8)$$

The eigenvalues are given by

$$\lambda_{mn} = \left(\frac{m\Pi}{b}\right)^2 + \left(\frac{n\Pi}{a}\right)^2 - k^2 \qquad (4.9)$$

Depending on the size of the cylinder relative to the wavenumber k, the operator may not be positive definite. In other words, for small cylinders all the

eigenvalues are positive-valued (and in fact lie far from the origin); as the cylinder size grows with respect to the wavelength the eigenvalues migrate to the left until the lowest crosses the origin onto the negative real axis. Thus, the operator may be indefinite for this problem. For a rectangular cylinder measuring one wavelength by two wavelengths in dimension, the smaller eigenvalues are listed in Table 4.2. (The operator is indefinite for the cylinder dimensions of Table 4.2.)

4.4 TM-wave scattering from circular cylinders

Consider the scattering of a time harmonic wave from a circular conducting cylinder of radius 'a.' The cylinder geometry is shown in Figure 4.2. If the excitation involves only the TM polarization (the electric field parallel to the cylinder), an appropriate equation is the electric-field integral equation (EFIE)[3]

$$E_z^{inc}(\phi) = L_{EFIE}^{TM}(J_z) = \frac{k\eta}{4} \int_{\phi'=0}^{2\pi} J_z(\phi') H_0^{(2)}(kR)\, a\, d\phi' \qquad (4.10)$$

where

$$R = 2a \left|\sin\left(\frac{\phi-\phi'}{2}\right)\right| \qquad (4.11)$$

E_z^{inc} denotes the source or "incident" field, and the parameters 'k' and 'η' describe the medium surrounding the cylinder.

In this case, the eigenfunctions of the integral operator are

$$\varepsilon_n(\phi) = e^{jn\phi} \qquad (4.12)$$

TABLE 4.2

EIGENVALUES OF THE HELMHOLTZ OPERATOR APPLIED TO A GROUNDED RECTANGULAR CYLINDER, FOR $a = 2$, $b = 1$ AND $k = 2\pi$.

m	n	λ_{mn}
1	1	- 27.141
1	2	- 19.739
1	3	- 7.402
2	1	2.467
1	4	9.870
2	2	9.870
2	3	22.207
1	5	32.076
2	4	39.478

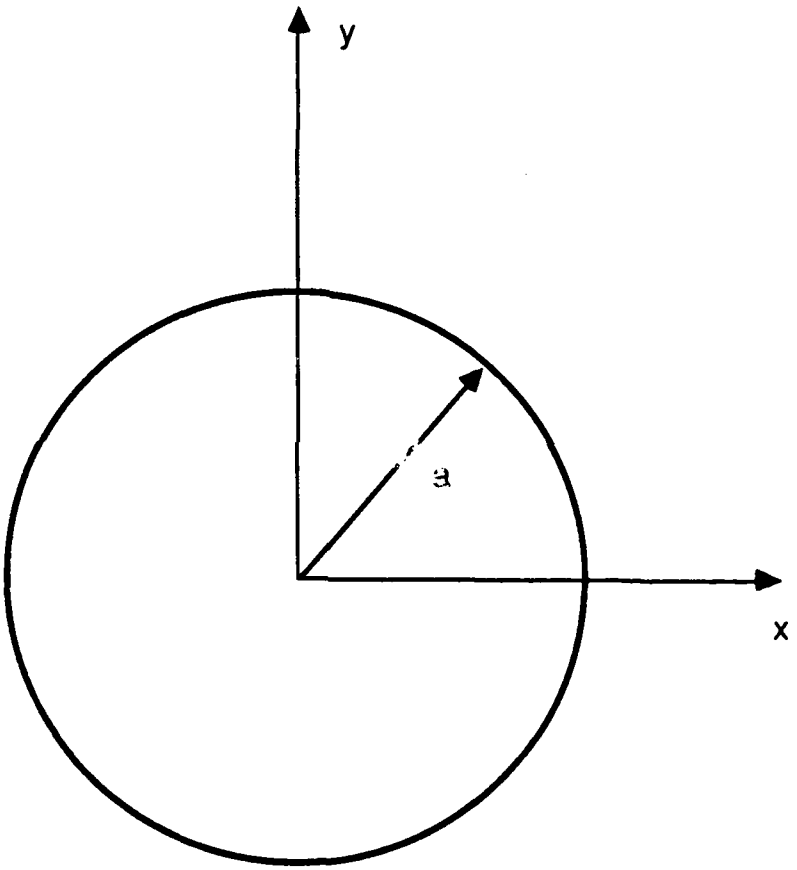

Figure 4.2 Geometry of circular cylinder.

and the corresponding eigenvalues are

$$\lambda_n^{TM,EFIE} = \frac{n\Pi ka}{2} J_n(ka)\, H_n^{(2)}(ka) \tag{4.13}$$

where J_n and H_n denote the n-th order Bessel and Hankel functions, respectively.

Note that the eigenvalues are complex-valued, and lie in the right-half complex plane, as illustrated in Table 4.3 for a cylinder having one wavelength circumference. As the cylinder circumference increases relative to the wavelength, the eigenvalues move around in the complex plane as illustrated in Figure 4.3. As can be seen from Figure 4.3, the eigenvalues may pass through the origin at certain values of 'ka' (at the zeros of the Bessel function J_n). For these values of 'ka,' the cylinder is a resonant cavity and the equation admits homogeneous (source-free) solutions[7,8]. The integral equation does not have a unique solution at these values of 'ka.'

Note that for very small cylinders, where $ka \to 0$,

$$\lambda_0^{TM} \sim \frac{n\Pi ka}{2}\left[1 - j\,\frac{2}{\Pi}\,\ell n\left(\frac{\gamma ka}{2}\right)\right] \to 0 \tag{4.14}$$

$$\lambda_n^{TM} \sim \frac{n\Pi}{n!}\left(\frac{ka}{2}\right)^{2n+1} + j\,\frac{\eta ka}{2n} \to 0, \quad n \neq 0 \tag{4.15}$$

and thus we can say that the eigenvalues cluster at the origin as the cylinder radius tends to zero. For very large cylinders, the eigenvalues behave according to

$$\lambda_0^{TM} \sim \eta \cos^2\left(ka - \frac{\pi}{4}\right) - j\,\eta \cos\left(ka - \frac{\pi}{4}\right)\sin\left(ka - \frac{\pi}{4}\right), \qquad ka \to \infty \tag{4.16}$$

Thus, the eigenvalues follow a circular path in the complex plane for asymptotically large cylinders.

TABLE 4.3

FIRST TEN DISTINCT EIGENVALUES OF THE EFIE OPERATOR

FOR A ONE WAVELENGTH CIRCUMFERENCE CYLINDER, TM POLARIZATION.

346.495 - j 39.964
114.592 + j 203.433
7.813 + j 112.240
0.226 + j 67.395
0.004 + j 48.773
0.0 + j 38.488
0.0 + j 31.854
0.0 + j 27.194
0.0 + j 23.735
0.0 + j 21.062

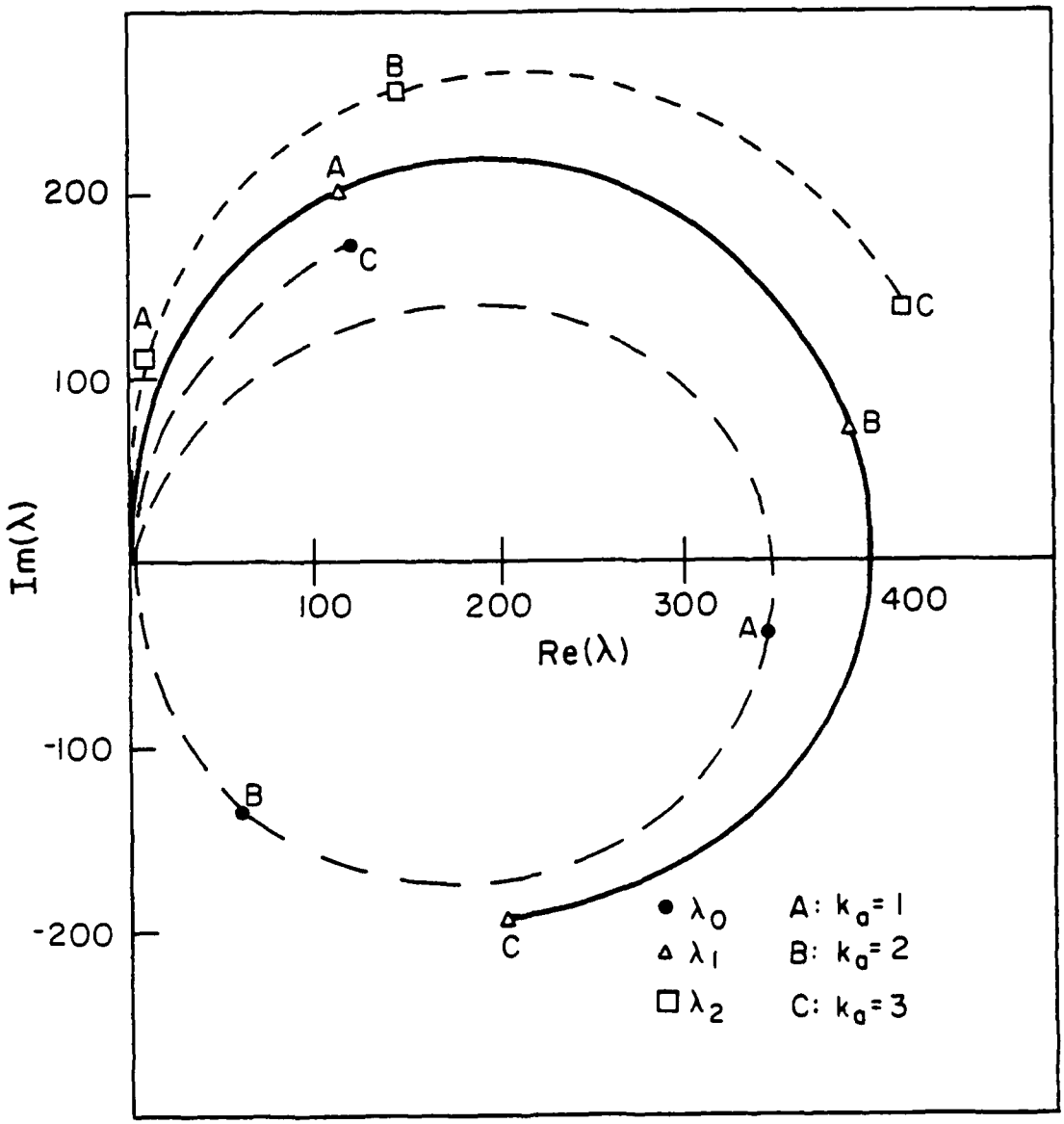

Figure 4.3 Trajectory of three eigenvalues of the TM EFIE applied to circular cylinders as a function of cylinder size ka.

4.5 TE-wave scattering from circular cylinders

In the previous example, the polarization of the incident electric field was assumed to be TM (parallel to the cylinder axis). If the polarization of the incident wave is TE (perpendicular to the axis of the cylinder), the EFIE takes the form[3]

$$E_{\phi}^{inc}(\phi) = L_{EFIE}^{TE}(J_{\phi}) = \frac{\eta}{4k}\,\hat{\phi}\cdot(\text{grad div} + k^2)\int_{\phi'=0}^{2\pi}\hat{\phi}(\phi')\,J_{\phi}(\phi')\,H_0^{(2)}(kR)\,a\,d\phi' \tag{4.17}$$

where R is defined in Equation (4.11). In this case, the eigenfunctions are

$$\epsilon_n(\phi) = e^{jn\phi} \tag{4.18}$$

and the corresponding eigenvalues are

$$\lambda_n^{TE,EFIE} = \frac{n\pi ka}{2}\,J_n'(ka)\,H_n^{(2)'}(ka) \tag{4.19}$$

where the primes denote differentiation with respect to the arguments of the Bessel and Hankel functions. Table 4.4 presents the dominant eigenvalues for a cylinder having one wavelength circumference.

Note that the eigenvalues are complex-valued and lie in the right-half plane, as was the case for the previous example involving the TM polarization. Again, they move around in the complex plane as the cylinder radius is increased relative to the wavelength, as illustrated in Figure 4.4. At certain values of 'ka,' an eigenvalue may vanish, and the EFIE has no unique solution for that cylinder geometry. However, the behavior of the eigenvalues is somewhat different from the previous example. Specifically, as the cylinder radius tends to zero,

TABLE 4.4

FIRST TEN EIGENVALUES OF THE EFIE OPERATOR

FOR A ONE WAVELENGTH CIRCUMFERENCE CYLINDER, TE POLARIZATION.

114.592 + j 203.43
62.562 - j 167.30
26.157 - j 313.54
1.870 - j 526.05
0.055 - j 727.42
0.001 - j 921.87
0.0 - j 1113.89
0.0 - j 1304.73
0.0 - j 1494.90
0.0 - j 1684.65

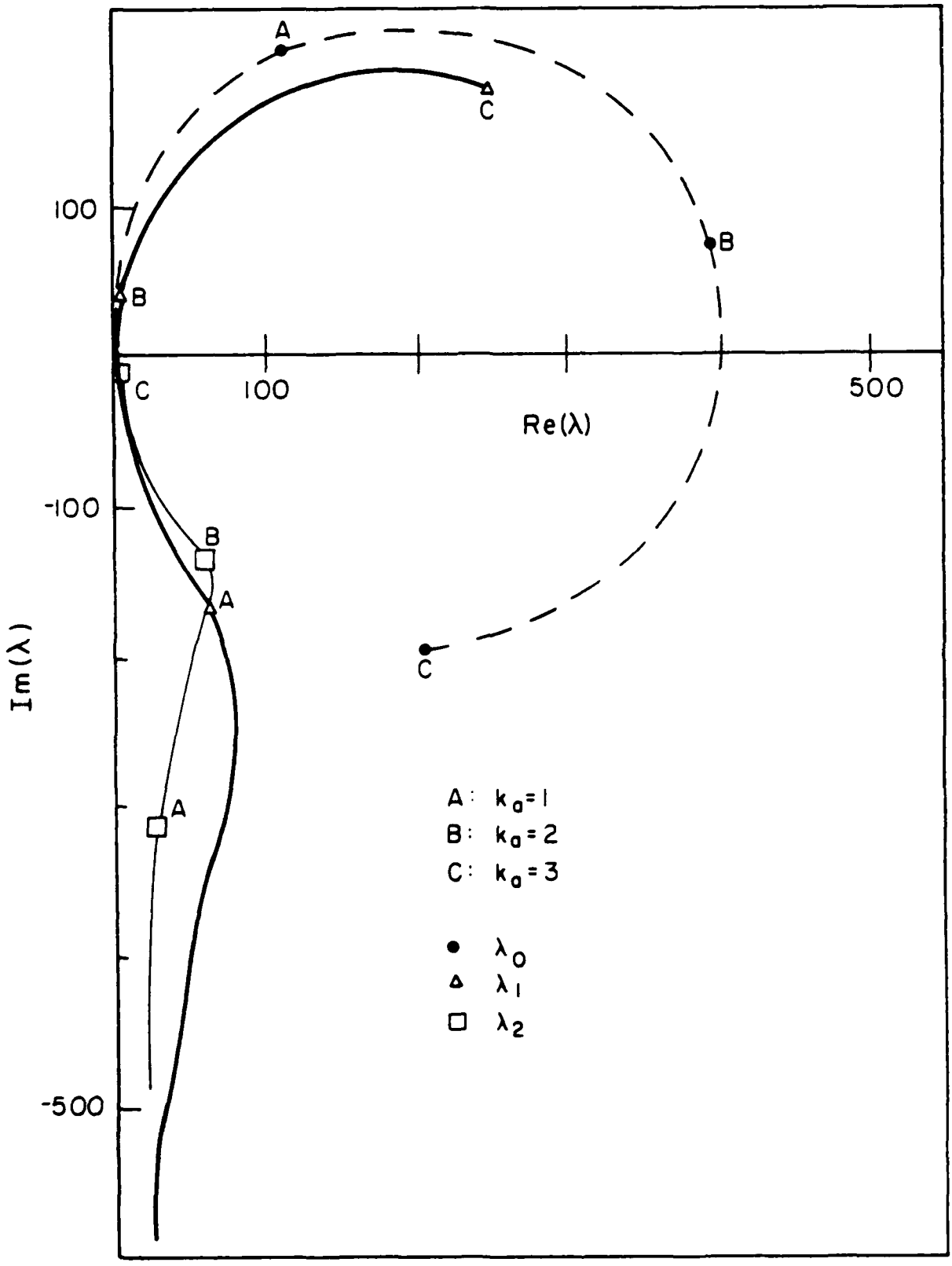

Figure 4.4 Trajectory of three eigenvalues of the TE EFIE applied to circular cylinders as a function of cylinder size ka.

$$\lambda_0 \to 0 \tag{4.20}$$

$$\lambda_n \to -j\,\infty \quad , \quad n \neq 0 \tag{4.21}$$

As the cylinder size increases asymptotically, eigenvalues follow a circular trajectory in the complex plane, much as those of the TM EFIE operator. However, the eigenvalues of this operator tend to cluster at infinity (again, speaking loosely) and are thus different in character from those of the TM EFIE operator.

4.6 Alternate formulation for TE-wave scattering

The previous example used the EFIE to represent TE-wave scattering from a conducting, circular cylinder. The same problem could be treated using an alternative formulation, the magnetic-field integral equation (MFIE). The MFIE for this problem is[3]

$$-H_z^{inc}(\phi) = L_{MFIE}^{TE}(J_\phi) = J_\phi + \frac{\hat{\phi}\cdot curl}{4j} \int_{\phi'=0}^{2\pi} \hat{\phi}(\phi')\, J_\phi(\phi')\, H_0^{(2)}(kR)\, a\, d\phi' \tag{4.22}$$

where R is defined in Equation (4.11) and H_z^{inc} denotes the incident magnetic field.

The eigenfunctions for this operator are

$$\epsilon_n(\phi) = e^{jn\phi} \tag{4.23}$$

and the corresponding eigenvalues are

$$\lambda_n^{TE,MFIE} = \frac{j\pi ka}{2} J_n(ka)\, H_n'(ka) \tag{4.24}$$

Table 4.5 shows the eigenvalues for a cylinder having one wavelength circumference.

The character of the MFIE eigenvalues is similar to those of the EFIE in certain respects. The eigenvalues are complex-valued and are located in the right-half complex plane. Figure 4.5 shows the movement of the dominant eigenvalues as the cylinder size is increased. Again, the eigenvalues may pass through the origin at certain values of 'a,' indicating cavity resonances and uniqueness problems for those cylinders. Similar to the EFIE operators, the eigenvalues follow a circular trajectory as the cylinder becomes asymptotically large.

However, as the cylinder radius tends to zero,

$$\lambda_0 \sim 1 - j\pi \left(\frac{ka}{2}\right)^2 + 1 \tag{4.25}$$

and

$$\lambda_n \sim \frac{1}{2} + j \frac{\pi}{2n!(n-1)!} \left(\frac{ka}{2}\right)^{2n} + \frac{1}{2} \tag{4.26}$$

Thus, the MFIE eigenvalues tend to cluster at 0.5 + j0 and 1 + j0 in the complex plane. This behavior is in contrast with the behavior of the eigenvalues of the two forms of the EFIE, which tend to cluster at the origin and at infinity, respectively.

4.7 Combined-field equation for TE-wave scattering

The EFIE and MFIE operators for TE-wave scattering from a conducting, circular cylinder are considered above. An alternate formulation involves the

TABLE 4.5

EIGENVALUES OF MFIE FROM EQ. (4.22)

FOR A ONE WAVELENGTH CYLINDER.

n	λ_n
0	0.93899 - j 0.52893
± 1	0.60100 + j 0.22475
± 2	0.45486 + j 0.03795
± 3	0.48596 + j 0.00173
± 4	0.49520 + j 0.00004
± 5	0.49775 + j 0.0
± 6	0.49875 + j 0.0
± 7	0.49923 + j 0.0

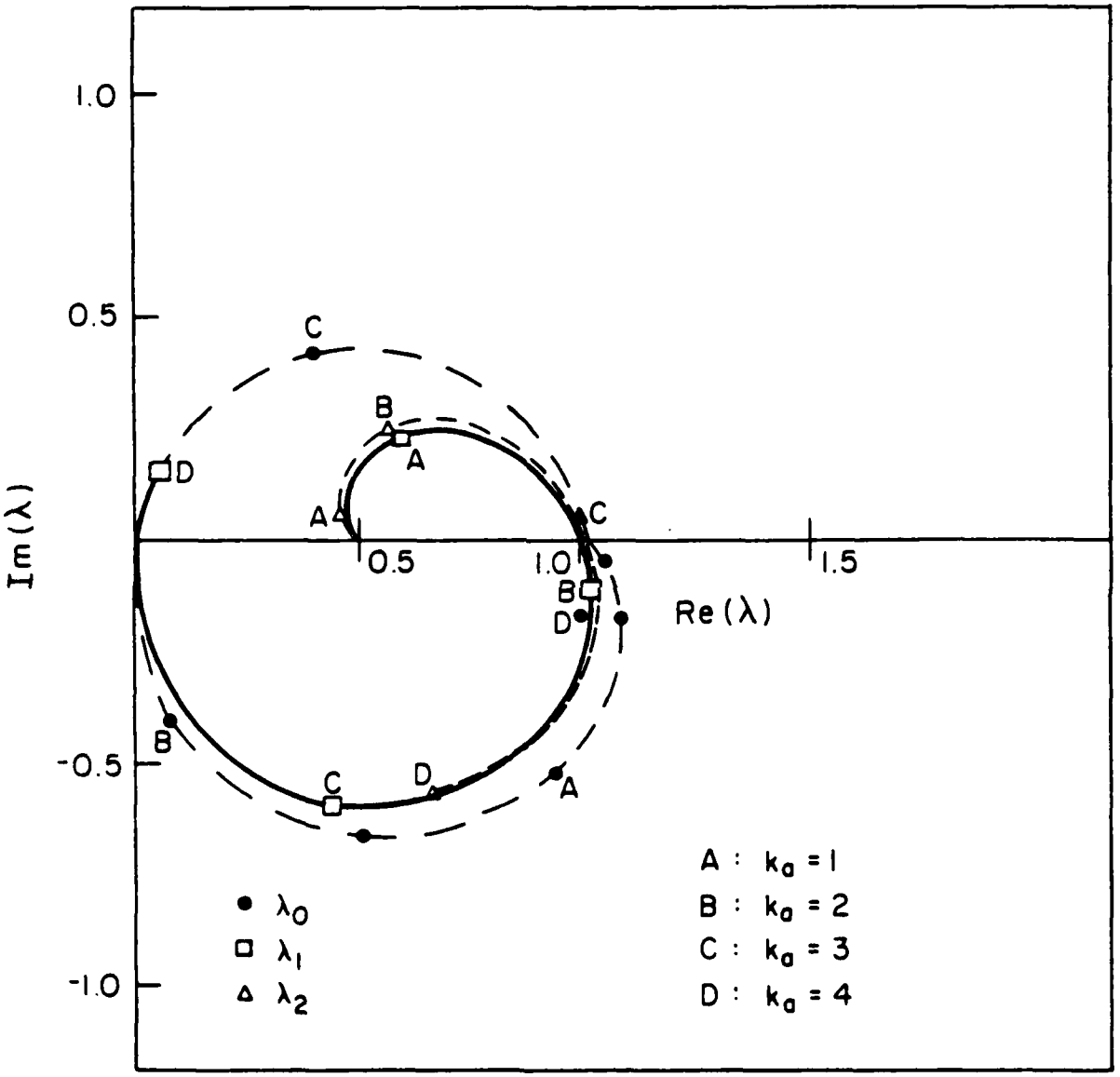

Figure 4.5 Trajectory of three eigenvalues of the TE MFIE applied to circular cylinders as a function of cylinder size ka.

combination of these operators and is known as the combined-field integral equation (CFIE)[8]

$$\alpha E_{\phi}^{inc}(\phi) - (1-\alpha)\,\eta\, H_z^{inc}(\phi) = L^{TE}_{CFIE}(\phi) = (1-\alpha)\,\eta\, J_{\phi}$$

$$+ \left[\alpha \frac{\eta}{4k}\,\hat{\phi}\cdot(\text{grad div} + k^2) + \frac{(1-\alpha)\eta}{4j}\,\hat{\phi}\cdot\text{curl}\right] \int_{\phi'=0}^{2\pi} \hat{\phi}(\phi')\, J_{\phi}(\phi')\, H_0^{(2)}(kR)\, a\, d\phi' \tag{4.27}$$

where R is defined in Equation (4.11), H_z^{inc} and E_{ϕ}^{inc} denote the incident magnetic and electric fields. The parameter α usually falls in the range between 0 and 1, and controls the weight of the electric and magnetic field operators in the CFIE.

The eigenfunctions for this operator are

$$\epsilon_n(\phi) = e^{jn\phi} \tag{4.28}$$

and the corresponding eigenvalues are

$$\lambda_n^{TE,CFIE} = \frac{n\pi ka}{2}\left[\alpha\, J_n'(ka) + j(1-\alpha)\, J_n(ka)\right] H_n^{(2)'}(ka) \tag{4.29}$$

Table 4.6 shows the eigenvalues for a cylinder having one wavelength circumference, for the case when the parameter α has the value 0.2. Figure 4.6 shows the movement of several of these eigenvalues as a function of cylinder size. Note that these eigenvalues do not pass through the origin, as do those of the EFIE and MFIE operators. The CFIE has unique solutions for all values of cylinder size, and thus may be preferred to the other formulations.

TABLE 4.6

EIGENVALUES OF THE CFIE OPERATOR
FROM EQ. (4.29) FOR A
1λ CIRCUMFERENCE CYLINDER, $\alpha = 0.2$.

n	λ_n
0	305.92 - j 118.72
± 1	193.65 + j 34.28
± 2	142.32 - j 51.27
± 3	146.83 - j 104.69
± 4	149.26 - j 145.47
± 5	150.02 - j 184.37
± 6	150.32 - j 222.78
± 7	150.46 - j 260.95
± 8	150.54 - j 298.98
± 9	150.59 - j 336.93

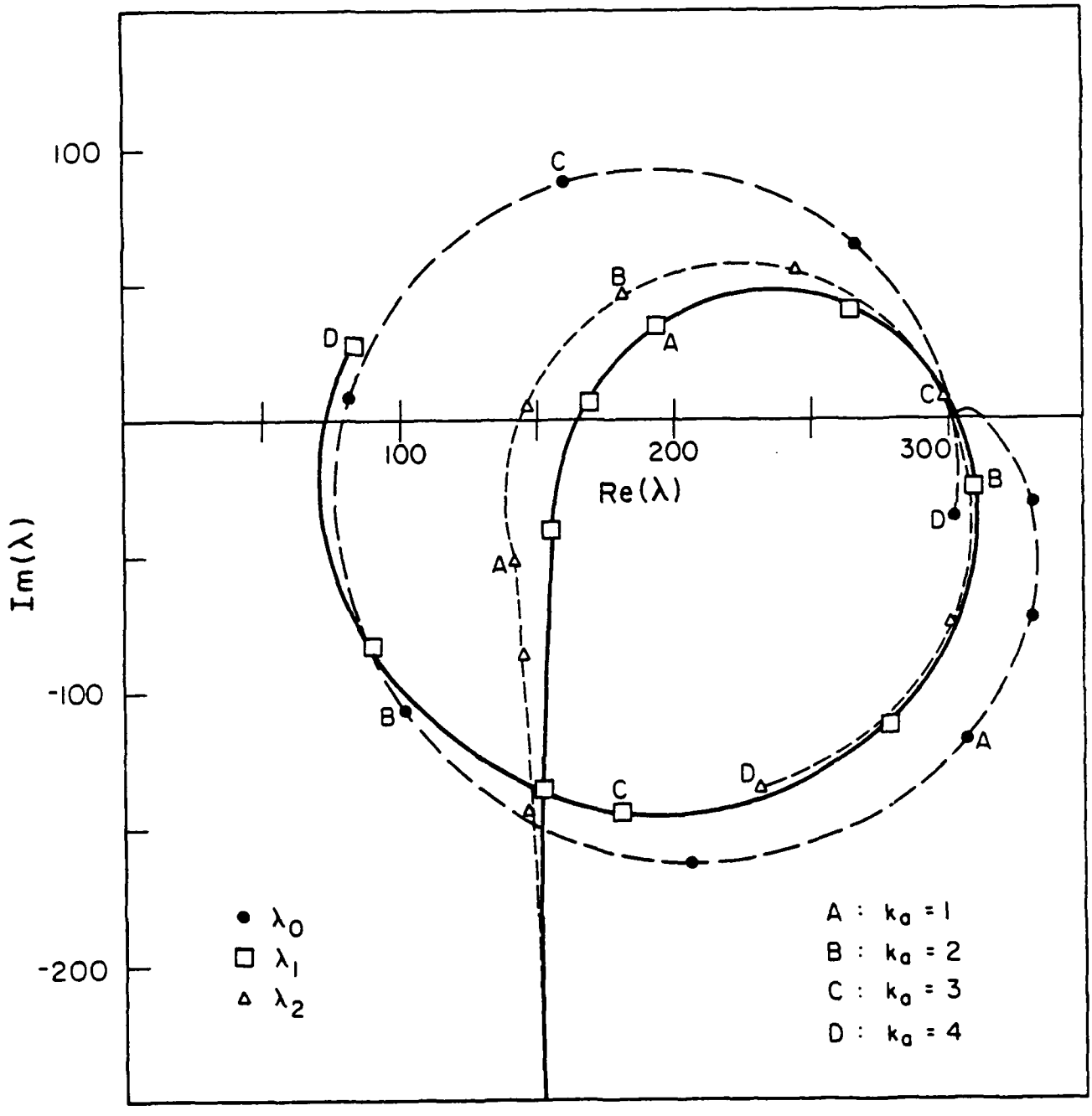

Figure 4.6 Trajectory of three eigenvalues of the TE CFIE applied to circular cylinders as a function of cylinder size ka.

4.8 Summary

A variety of examples of electromagnetic field problems have been investigated to illustrate the type of eigenvalue spectrum arising in practice. The theory of Chapter 2 can be used to relate the eigenvalue spectrum of the continuous operator equation to that of the corresponding matrix equation. Since these examples can all be treated analytically, they permit the theory to be tested in a controlled manner. Chapter 5 will examine these examples again, from a numerical implementation, and test the theory of Chapter 2 in each case.

5. EIGENVALUE SPECTRUM OF MATRIX OPERATORS

Chapters 2 and 3 presented a theory relating the eigenvalues of a continuous operator to those of the finite-difference, finite-element, or method-of-moments matrix. To verify the theory, this chapter compares numerical eigenvalues from such matrices with eigenvalues of continuous operators previously tabulated in Chapter 4.

The two-dimensional Poisson equation describing the potential within a grounded conducting cylinder containing free charge density is presented in Equation (4.2). The geometry is displayed in Figure 4.1. The eigenvalues of the continuous operator equation for a cylinder geometry of dimension a=2, b=1 are presented in Table 4.1. Consider a matrix approximation to this operator based on a finite-difference method (FDM) using conventional central-differencing formulas[1]. The same matrix could be obtained from the MoM using the basis and testing functions of Equations (3.21) and (3.22). In either case, the matrix elements have the form

$$\ell_{mn} = \begin{cases} -\dfrac{4}{\Delta^2} & m = n \\ \dfrac{1}{\Delta^2} & m, n \text{ represent adjacent grid points} \\ 0 & \text{otherwise} \end{cases} \qquad (5.1)$$

where Δ is the interval between grid points (centers of the basis/testing functions in the context of the MoM). According to the eigenvalue projection theory of Chapter 2, the eigenvalues of the continuous operator should be approximated by the eigenvalues of the matrix

$$\underline{\underline{S}}^{-1}\,\underline{\underline{L}} \tag{5.2}$$

where the elements of the scaling matrix are given by

$$S_{mn} = \begin{cases} \frac{7}{12} & m = n \\ \frac{1}{12} & m,n \text{ represent adjacent grid points} \\ \frac{1}{48} & m,n \text{ represent adjacent corner grid points} \\ 0 & \text{otherwise} \end{cases} \tag{5.3}$$

Table 5.1 presents a comparison of the smallest eigenvalues of the FDM matrix and those of the continuous operator for several different levels of discretization. The numerical eigenvalues appear to be converging to those of the continuous operator as the order of the discretization is increased.

The Helmholtz equation describing a rectangular geometry is presented in Equation (4.6) and eigenvalues of the operator are tabulated in Table 4.2. The elements of a modified FDM matrix are presented in Equation (3.23). The elements of the scaling matrix used for this case are those given in Equation (5.3). Table 5.2 compares the eigenvalues of the FDM matrix with those of the continuous operator from Table 4.2. Again, the matrix eigenvalues appear to converge toward the continuous eigenvalues as the order of the matrix is increased.

The electric-field integral equation (EFIE) describing the scattering of a TM wave from a circular cylinder is presented in Equation (4.10). A matrix approximation to this operator can be based on the use of pulse basis functions

TABLE 5.1

SMALLEST SIX EIGENVALUES OF $\underline{\underline{S}}^{-1}\underline{\underline{L}}$ COMPARED TO THOSE OF THE POISSON OPERATOR FOR a = 2, b = 1.

21 × 21 matrix	55 × 55 matrix	105 × 105 matrix	Poisson Operator from Table 4.1
+ 12.98	+ 12.63	+ 12.50	12.34
+ 21.78	+ 20.64	+ 20.25	19.74
+ 36.99	+ 34.28	+ 33.32	32.08
+ 46.70	+ 44.31	43.31	41.95
+ 59.00	+ 53.89	51.93	49.35
+ 59.00	+ 53.89	51.93	49.35

TABLE 5.2

SMALLEST SEVEN EIGENVALUES OF $\underline{\underline{S}}^{-1}\underline{\underline{L}}$ COMPARED TO THOSE OF THE HELMHOLTZ OPERATOR, FOR a = 2, b = 1, k = 2π.

21 × 21	55 × 55	105 × 105	Helmholtz operator Table 4.2
- 26.50	- 26.85	- 26.98	- 27.141
- 17.70	- 18.83	- 19.23	- 19.739
- 2.49	- 5.20	- 6.16	- 7.402
7.23	4.83	+ 3.83	2.467
+ 19.53	14.41	12.45	9.870
19.53	14.41	12.45	9.870
40.50	30.66	26.98	22.207

and Dirac delta testing functions, according to

$$B_n(\ell) = p(\ell;\ \ell_n - \frac{\Delta}{2},\ \ell_n + \frac{\Delta}{2}) \tag{5.4}$$

$$T_m(\ell) = \delta(\ell - \ell_m) \tag{5.5}$$

The basis and testing functions have been defined in Figure 3.1.

For the basis and testing functions defined in Equations (5.4) and (5.5), the scaling matrix defined in Equation 2.12 is an identity matrix. As a result, the eigenvalues of the matrix $\underline{\underline{L}}$ should be a direct approximation to those of the original EFIE operator. Table 5.3 presents a comparison of the dominant eigenvalues of the matrix operator for a system of order 30. The matrix eigenvalues closely approximate those of the continuous operator.

For the EFIE representing a TE wave incident upon a circular cylinder (Equation (4.17)), and the MoM matrix based on the basis and testing functions

$$B_n(\ell) = t(\ell;\ \ell_n - \Delta,\ \ell_n,\ \ell_n + \Delta) \tag{5.6}$$

$$T_m(\ell) = \frac{1}{\Delta}\, p(\ell;\ \ell_m - \frac{\Delta}{2},\ \ell_m + \frac{\Delta}{2}) \tag{5.7}$$

the scaling matrix contains the entries

$$S_{mn} = \begin{cases} \frac{3}{4} & m = n \\ \frac{1}{8} & m,n \text{ represent adjacent cells in the model} \\ 0 & \text{otherwise} \end{cases} \tag{5.8}$$

Table 5.4 presents a comparison of the eigenvalues of the matrix operator $\underline{\underline{S}}^{-1}\underline{\underline{L}}$,

TABLE 5.3

FIRST ELEVEN DISTINCT EIGENVALUES OF THE EFIE OPERATOR COMPARED TO THOSE OF THE MOMENT METHOD MATRIX OPERATOR FOR A ONE WAVELENGTH CIRCUMFERENCE CYLINDER, TM POLARIZATION.

EFIE (Eq. (4.13))	30 × 30 matrix
346.495 - j 39.964	346.43 - j 41.59
114.592 + j 203.433	114.55 + j 201.56
7.813 + j 112.240	7.820 + j 110.35
0.226 + j 67.395	0.232 + j 65.62
0.004 + j 48.773	0.004 + j 47.08
0.0 + j 38.488	0.010 + j 36.96
0.0 + j 31.854	0.018 + j 30.51
0.0 + j 27.194	0.020 + j 26.13
0.0 + j 23.735	0.001 + j 23.02
0.0 + j 21.062	- 0.007 + j 20.82
0.0 + j 18.932	- 0.004 + j 19.04

TABLE 5.4

FIRST ELEVEN EIGENVALUES OF THE EFIE COMPARED TO THOSE OF THE MOMENT-METHOD $\underline{\underline{L}}$-MATRIX AND THE PRODUCT MATRIX $\underline{\underline{S}}^{-1}\underline{\underline{L}}$ FOR A ONE WAVELENGTH CIRCUMFERENCE CYLINDER, TE POLARIZATION. THE ORDER OF $\underline{\underline{S}}$ AND $\underline{\underline{L}}$ IS 30.

EFIE (Eq. (4.19))	$\underline{\underline{L}}$-matrix	$\underline{\underline{S}}^{-1}\underline{\underline{L}}$-matrix
114.592 + j 203.43	111.6 + j 200.1	112.2 + j 201.1
62.562 - j 167.30	61.7 - j 166.6	62.4 - j 168.4
26.157 - j 313.54	25.6 - j 306.4	26.3 - j 314.9
1.870 - j 526.05	1.83 - j 500.5	1.93 - j 528.5
0.055 - j 727.42	0.05 - j 668.9	0.06 - j 733.2
0.001 - j 921.87	0.0 - j 813.0	0.0 - j 934.3
0.0 - j 1113.9	0.0 - j 935.6	0.0 - j 1137
0.0 - j 1304.7	0.0 - j 1037	0.0 - j 1344
0.0 - j 1494.9	0.0 - j 1120	0.0 - j 1555
0.0 - j 1684.7	0.0 - j 1185	0.0 - j 1770
0.0 - j 1874.1	0.0 - j 1234	0.0 - j 1984

the matrix operator $\underline{\underline{L}}$, and the continuous operator of Equation (4.17). The scaled eigenvalues are a better approximation to those of the continuous operator than are those of the matrix $\underline{\underline{L}}$.

Several examples have been presented that compare the eigenvalues of continuous operators to those of the associated MoM or FDM matrices. These examples are intended to confirm the theory presented in Chapters 2 and 3, and in addition provide a framework for the future study of the eigenvalue spectrum of other operator equations. In cases where eigenvalues are not available from analytical means, those of the matrix $\underline{\underline{S}}^{-1}\underline{\underline{L}}$ can be used to estimate the spectrum of the original continuous operator. This procedure may be important for the study of typical eigenvalue spectrums, as few continuous operators arising from practical electromagnetics applications yield analytical expressions for eigenvalues.

6. APPLICATIONS OF THE EIGENVALUE PROJECTION THEORY TO MATRIX CONDITIONING AND THE CONVERGENCE OF ITERATIVE ALGORITHMS

The eigenvalue projection theory presented in previous chapters has a direct bearing on several applications of current interest. One issue involves the basis and testing functions used to discretize a continuous equation and their effect on the condition number of the resulting matrix equation. If possible, it is desirable to select basis and testing functions in order to achieve a well-conditioned matrix representation. Knowledge of the eigenvalue spectrum and its behavior for limiting cases may be also useful for the identification of regions of numerical instability. For instance, certain numerical formulations fail when applied to electrically small geometries. An additional issue involves the choice of solution algorithms: if an iterative procedure is employed to solve the matrix equation, knowledge of the typical eigenvalue spectrum can provide information essential to the choice of a convergent algorithm.

The relation between the eigenvalues of the original operator and the condition number of the $\underline{\underline{L}}$-matrix obtained from the MoM procedure is delineated in Chapter 2. Since the eigenvalues of the continuous operator are fixed by the specific equation and geometry of interest, the only control over the condition number of the $\underline{\underline{L}}$-matrix is provided through the choice of basis and testing functions. Since the eigenvalues of the product matrix $\underline{\underline{S}}^{-1}\underline{\underline{L}}$ approximate those of the original operator, the condition number of $\underline{\underline{S}}^{-1}\underline{\underline{L}}$ should be independent of the basis and testing functions. This suggests that the matrices $\underline{\underline{S}}$ and $\underline{\underline{L}}$ will tend to compensate for each other. If $\underline{\underline{S}}$ is poorly conditioned, $\underline{\underline{L}}$ may also be poorly

conditioned in order that $\underline{\underline{S}}^{-1}\underline{\underline{L}}$ have a spectrum in agreement with that of the original operator. As a general rule, basis and testing functions should be selected in order to produce a well-conditioned scaling matrix $\underline{\underline{S}}$. For example, the $\underline{\underline{S}}$-matrix produced by the use of subsectional pulse basis functions and Dirac delta testing functions is often an identity matrix, and is perfectly conditioned. On the other hand, the use of entire-domain basis functions can lead to a very ill-conditioned $\underline{\underline{S}}$-matrix (see p. 410 of [9]). Entire-domain functions are often associated with poorly conditioned $\underline{\underline{L}}$-matrices.

Suppose the continuous operator is such that the eigenvalue spectrum excited by the right-hand side of the equation involves eigenvalues having very large and small magnitudes. Such an equation will be difficult to treat numerically, as the $\underline{\underline{L}}$-matrix will be poorly conditioned regardless of the condition number of $\underline{\underline{S}}$. In this type of situation, knowledge of the eigenvalue spectrum may motivate the search for an alternative formulation. An example involving a poorly conditioned system can be drawn from the equations discussed in Chapter 4. The EFIE used for TE-wave scattering from circular cylinders is presented in Equation (4.17), and the associated eigenvalues appear in Equation (4.19). Note that as the cylinder radius decreases with respect to the wavelength, the eigenvalues spread in the complex plane according to Equations (4.20) and (4.21). It has been observed that the numerical solution to the TE EFIE is numerically unstable for electrically small cylinders[10]. An alternative formulation, the TE MFIE presented in Equation (4.22), remains stable as the cylinder size decreases. Note that the TE MFIE eigenvalues do not spread as the cylinder size is decreased, but cluster in reasonable proximity to each other.

In recent years, a considerable effort has been directed toward the implementation of iterative solution algorithms for treating certain electromagnetic scattering problems[11]. A variety of integral equation formulations yield matrices having special structure in the form of slightly perturbed Toeplitz symmetries[12,13]. Iterative algorithms have been used to exploit this structure and permit the analysis of geometries that are electrically larger than those solvable by other techniques. However, simple iterative algorithms sometimes diverge when applied to the general complex-valued matrices arising from electromagnetics problems[14,15].

Information concerning the typical matrix eigenvalue spectrum encountered in these systems can be used to select a suitable iterative algorithm for the problem at hand. For example, it is well known that the Jacobi algorithm requires the eigenvalues of the iteration matrix to lie within the unit circle centered at 1+j0 in the complex plane[5]. The eigenvalues of the TE MFIE discussed in Chapter 4 appear to satisfy this criterion, at least for the case of a circular cylinder. However, the EFIE formulations presented in Chapter 4 do not satisfy this condition. Therefore, it is expected that the Jacobi algorithm may be divergent for systems representing the EFIE formulation. (Note that the iteration matrix arising within the Jacobi algorithm is not necessarily the L-matrix discussed above, but generally involves a splitting and subsequent scaling in an attempt to shift the eigenvalues into the necessary interval[5].) Other iterative algorithms are capable of treating systems with eigenvalues distributed throughout the right-half complex plane, but require some knowledge concerning eigenvalue location in order to assure convergence[16]. Algorithms that permit the user to specify parameters to accelerate the convergence rate can use apriori knowledge of the eigenvalue spectrum to optimize these parameters.

7. CONCLUSIONS

An eigenvalue projection theory is presented that relates the eigenvalue spectrum of continuous operators to the eigenvalues of the matrix operator arising from a MoM or FEM discretization. An approximate equivalence between the FDM and MoM procedures is developed which permits the theory to be applied to FDM matrices. Numerical examples are used to confirm the theory for integral and differential equations, and to illustrate the typical eigenvalue spectrum arising from electromagnetics equations.

Knowledge of the eigenvalue spectrum aids in the selection of robust problem formulations and discretization procedures. If an iterative algorithm is used to obtain the solution, such knowledge can also be used to optimize the algorithm's convergence behavior to the problem of interest.

8. REFERENCES

[1] G. D. Smith, Numerical Solution of Partial Differential Equations: Finite Difference Methods. New York: Oxford University Press, 1978.

[2] P. P. Silvester and R. L. Ferrari, Finite Elements for Electrical Engineers. Cambridge: Cambridge University Press, 1983.

[3] R. F. Harrington, Field Computation by Moment Methods. Malabar, FL: Krieger, 1982.

[4] D. J. Evans, ed. Preconditioning Methods: Analysis and Applications. New York: Gordon and Breach, 1983.

[5] R. S. Varga, Matrix Iterative Analysis. Englewood Cliffs: Prentice-Hall, 1962.

[6] S. G. Mikhlin, Variational Methods in Mathematical Physics. New York: Macmillan, 1964.

[7] R. Mittra and C. A. Klein, "Stability and convergence of moment method solutions," in Numerical and Asymptotic Techniques in Electromagnetics, ed. R. Mittra. New York: Springer-Verlag, 1975.

[8] J. R. Mautz and R. F. Harrington, "H-field, E-field and combined-field solution for conducting bodies of revolution," AEU, vol. 32, pp. 157-163, 1978.

[9] J. R. Mautz and R. F. Harrington, "Radiation and scattering from bodies of revolution," Appl. Sci. Res., vol. 20, pp 405-435, June 1969.

[10] J. R. Mautz and R. F. Harrington, "An E-field solution for a conducting surface small or comparable to the wavelength," IEEE Trans. Antennas Propagat., vol. AP-27, pp. 330-339, April 1984.

[11] A. F. Peterson, "Iterative methods: when to use them for computational electromagnetics," Applied Computational Electromagnetics Newsletter, vol. 2, pp. 43-52, May 1987.

[12] A. F. Peterson and R. Mittra, "On the implementation and performance of iterative methods for computational electromagnetics," UILU-ENG-85-2571, Electromagnetic Communication Laboratory, University of Illinois, Urbana, IL, 1985.

[13] A. F. Peterson and R. Mittra, "Iterative based computational methods for electromagnetic scattering from individual or periodic structures," IEEE J. Oceanic Engineering, vol. OE-12, 1987 (in press).

[14] M. F. Sultan and R. Mittra, "Iterative methods for analyzing the electromagnetic scattering from dielectric bodies," UILU-ENG-84-2541, Electromagnetics Laboratory, University of Illinois, Urbana, IL, 1984.

[15] S. Ray and R. Mittra, "Spectral-iterative analysis of radiation and scattering problems," UILU-ENG-84-2550, Electromagnetic Communication Laboratory, University of Illinois, Urbana, IL, 1984.

[16] T. A. Manteuffel, "The Tchebyshev iteration for nonsymmetric linear systems," Numer. Math., vol. 28, pp. 307-327, 1977.

END

11-87

DTIC